Macromolecules

COMMUNICATION TO THE EDITOR

pubs.acs.org/Macromolecules

2,3-*exo*-Disyndiotactic Polynorbornene: A Crystalline Polymer with Tubular Helical Molecular Structure

Annamaria Buono,[†] Antonino Famulari,[†] Stefano Valdo Meille,*[,†] Giovanni Ricci,[‡] and Lido Porri*[,†]

[†]Dipartimento di Chimica, Materiali e Ingegneria Chimica "G. Natta" Politecnico di Milano, Piazza Leonardo da Vinci 32, I-20133 Milano, Italy

[‡]CNR-Istituto per lo Studio delle Macromolecole (ISMAC), Via E. Bassini 15, I-20133 Milano, Italy

Supporting Information

INTRODUCTION

Norbornene (NB) has been polymerized by many catalysts, and different types of polymers have been obtained.[1] Of particular interest is vinyl-type polynorbornene (PNB), which has industrial relevance for optical and electronic applications. Most of the catalysts so far identified for the vinyl-type polymerization of NB give polymers that are amorphous because of their low tacticity.[1] The ^{13}C NMR spectra of these polymers are consistent with a *cis-exo*-2,3 monomer insertion and indicate that *mm*, *mr*, and *rr* triads are present in different proportions depending on the catalyst used. Crystalline polymers, however, have been obtained with some catalysts: Al(*i*-Bu)$_3$−TiCl$_4$,[2] zirconocene−MAO (MAO = methylalumoxane),[3] and various chromium catalysts.[4] In contrast to previous proposals, crystallographic studies on oligomers, as well as NMR and modeling studies, have recently shown that the polymerization process of zirconocene−polynorbornene involves, along with *cis-exo*-2,3 insertions, also C7 linkages formed as a result of a σ-bond metathesis reaction.[5] A novel structure has been proposed for the resulting polymer, whose crystallinity has not been mentioned or described and which cannot be considered simply a vinyl-type PNB.[5] Among PNBs obtained from chromium catalysts,[4] only the polymer from MAO−CrCl$_2$(dppa)[4d] was characterized structurally: it was recently reported that it contains stereoregular sequences of *mr* triads which adopt regular, low-energy conformations allowing some degree of crystallization.

As mentioned above, a crystalline PNB was obtained in 1963 with Al(*i*-Bu)$_3$−TiCl$_4$, at Al/Ti molar ratio about 0.5.[2] The polymer was reported to be soluble in hydrocarbon solvents, but its structure was not investigated. Metathesis reactions of the kind observed with zirconocene catalysts are less common with Ti catalysts,[6] and therefore it appears of interest to examine the structure of polynorbornene obtained with TiCl$_4$-based catalysts. Because of their high crystallinity, these polymers are plausibly stereoregular and amenable not only to modeling and solution spectroscopy but also to X-ray diffraction investigations. In a previous Note[7] we reported on the oligomerization of norbornene using the same AlEt$_2$Cl-TiCl$_4$ catalyst system at a monomer/TiCl$_4$ molar ratio of about 11. Along with other oligomers, a crystalline heptamer was obtained with a stereoregular 2,3-*exo*-disyndiotactic structure. In the present note we report that the crystalline fractions obtained at high monomer/TiCl$_4$ ratio, under the same conditions, consist of polymers having a 2,3-*exo*-disyndiotactic structure.[7] Using molecular modeling methods combined with structural analysis based on X-ray diffraction spectra, we have found that the polymer chains adopt in the crystal a helical conformation with unique structural features for polymeric materials.

RESULTS AND DISCUSSION

Polymer Preparation and Characterization. The polymerization of norbornene was examined at different NB/TiCl$_4$ molar ratios as summarized in Table 1, while more detailed data are reported in the Supporting Information. Fully saturated vinyl addition polymers or oligomers were obtained, as indicated by the fact that in the olefinic region of their ^{1}H spectra no signals were observed. This evidence was confirmed by the absence of bands in the 1680−1620 cm^{-1} region in their IR spectra.[4a] The effect of monomer/TiCl$_4$ molar ratio on the structure of the crystalline fraction is evident from the results of two polymerization runs carried out with AlEt$_2$Cl−TiCl$_4$ at monomer/Ti molar ratio 11 (typical for the formation of the heptamer)[7] and 18, respectively. The products were fractionated by extraction with boiling ether, which dissolves low oligomers and the amorphous fraction, and then with boiling toluene, which dissolves part of the crystalline fraction. Figure 1b,c shows the X-ray powder spectra of the crystalline fractions (residue to the extraction) obtained in two polymerization runs (see Table 1, runs 1 and 2). The diffraction pattern of Figure 1a (NB/TiCl$_4$ molar ratio 11) is that of the heptamer;[7] that of Figure 1b (NB/TiCl$_4$ molar ratio 18) is quite different and clearly indicates the formation of a new crystalline phase. The molecular weight of the species giving rise to the new phase, as determined for the fraction soluble in boiling toluene by gel permeation chromatography (GPC), is about 1500, which means that it is a mixture of oligomers having average degree of polymerization of about 15. It appears highly plausible from the mode of formation that the new, higher crystalline oligomers of NB have a 2,3-*exo*-disyndiotactic structure as the heptamer. Actually, they are obtained with the same catalyst, under the same polymerization conditions; only the monomer/TiCl$_4$ ratio has been varied from 11 to 18. Such a modest variation in the monomer/catalyst ratio cannot affect the catalyst stereospecificity.

Received: March 3, 2011
Revised: April 12, 2011
Published: April 22, 2011

Table 1. Polymerization of Norbornene (NB) with $TiCl_4$−$AlEt_2Cl$[a]

	polymerization		polymer fractionation								
			diethyl ether-soluble fraction			toluene-soluble fraction			toluene-insoluble residue		
run	NB (g)	NB/Ti (molar ratio)	(%)	M_w	M_w/M_n	(%)	M_w	M_w/M_n	(%)	M_w	M_w/M_n
1	3.38	18	70.1	965	1.2	18.0	1489	1.2	11.9		
2	4.69	250	43.6	1135	1.4	22.1	4372	1.4	34.3		

[a] Polymerization conditions: heptane, total volume 12 mL; $AlEt_2Cl/Ti$ molar ratio = 2; $TiCl_4$, 2 mmol (0.2 mmol in run 2); polymerization temperature, 0 °C; polymerization time, 24 h; monomer conversion, 100%.

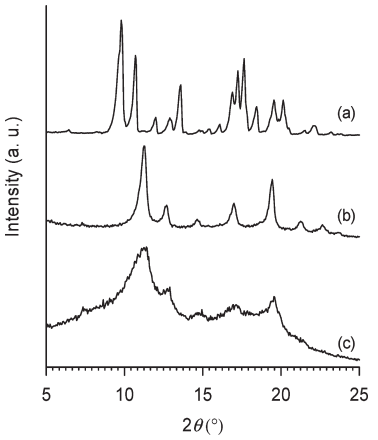

Figure 1. Experimental X-ray diffraction patterns of (a) the 2,3-*exo*-disyndiotactic heptamer (see ref 7) and of the toluene-insoluble residues (see text for details) obtained in runs 1 (b) and 2 (c) and described in Table 1 and in the Supporting Information.

Products with a much higher molecular weight are obtained by increasing the NB/$TiCl_4$ molar ratio. The polymerization product obtained at NB/$TiCl_4$ of 250 (see Table 1) consists of an amorphous fraction (43.6% of the total) soluble in diethyl ether, a crystalline fraction soluble in boiling toluene (22.1%) and a residue to toluene extraction. The crystalline fraction soluble in boiling toluene has M_w about 4400, and it exhibits the same X-ray powder diffraction pattern (not shown) as the products obtained at NB/$TiCl_4$ molar ratio 18 (Figure 1b), which means that the two products have the same stereochemical structure. The residue to the toluene extraction (about 34% of the total) exhibits an X-ray powder diffraction pattern (Figure 1c) displaying crystalline maxima which are broader but at the same 2θ positions as those in the pattern of the toluene extract. Profile c in Figure 1 also indicates the presence of a significant amorphous component in the residue, whose molecular weight is quite probably higher than that of the toluene extract but could not be determined because of its insolubility.

The close similarity of the diffraction patterns of the crystalline component of the products obtained with NB/$TiCl_4$ ratios ≥18 strongly suggests that a single phase of the same stereoregular polymer forms in all the above-discussed instances. Moreover, the ^{13}C NMR spectrum of the toluene extracts of the new crystalline polymer (see Supporting Information, ^{13}C NMR spectra in Figure 1S) clearly indicates a different stereochemistry with respect to the crystalline 2,3-*exo*-diheterotactic polynorbornene obtained with chromium catalysts.[4d]

Structural Analysis. Our analysis concentrated essentially on the 2,3-*exo*-disyndiotactic stereochemistry, on the basis of the considerations reported in the previous section. A schematic representation of a fully extended 2,3-*exo*-disyndiotactic PNB (dsPNB) chain showing stereochemical details is reported in Figure 2. Considerations involving the symmetry elements allowed by this stereochemistry guided us in the model building process. Glide-plane conformations and helical conformations were considered: in the latter case helix residues must consist, as in other syndiotactic polymers, of an even number of monomer units. The sequence of inter-ring torsion angles in the crystalline heptamer,[7] namely 88.5°, −149.8°, 89.6°, −133.0°, 166.6°, and −68.0°, provided useful hints, although hardly applicable

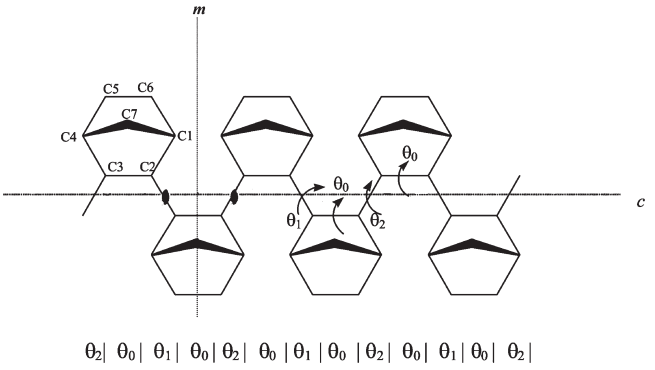

Figure 2. Sketch of the extended dsPNB chain showing stereochemical details and intrachain symmetry elements that may in principle apply.

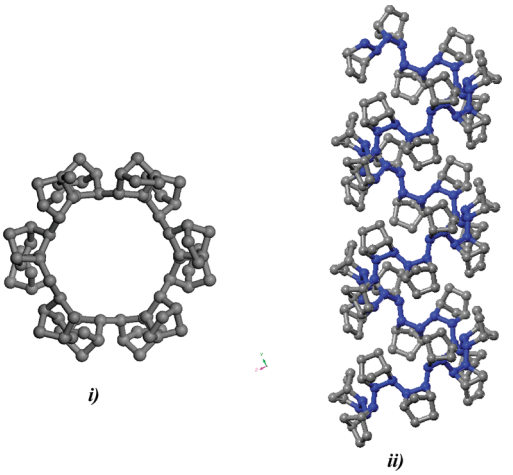

Figure 3. Projection views (i) down the chain axis and (ii) lateral of the lowest energy dsPNB isolated chain model. The polymer displays 6_1 helical symmetry with two monomers, related by 2-fold axes orthogonal to the chain axis, in each helix residue.

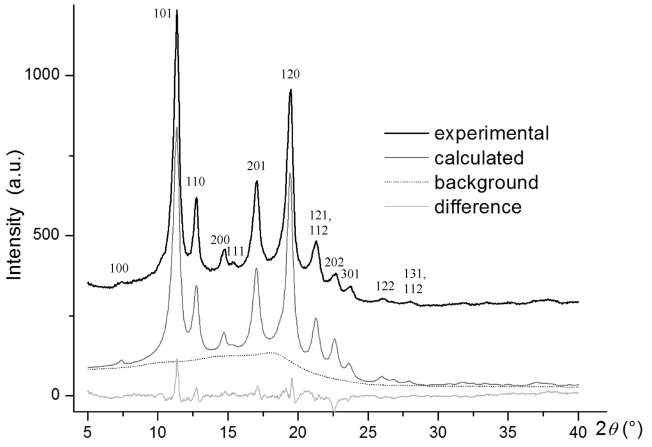

Figure 4. Experimental (continuous line) X-ray diffraction pattern of a typical 2,3-*exo*-disyndiotactic polynorbornene sample (toluene insoluble residue) showing also the indexing of the main contributing reflections. The calculated profile (dark gray) for the $P6_1$ model containing toluene guest molecules, the baseline (dotted line) used as background, and the difference curve (light gray) are also shown. The final disagreement factor was of 0.117 while refined cell parameters are $a = b = 14.10$ Å and $c = 10.44$ Å.

without substantial alterations to a periodic polymer in a crystalline phase.

Extensive work using the Materials Studio suite of programs[8] led us to identify a molecular model for the 2,3-*exo*-disyndiotactic polymer chain with particularly low energy. It is characterized by a 6_1 helical symmetry, and it is displayed in Figure 3. Because of its effectiveness in the structural modeling of 2,3-*exo*-diheterotactic PNB[4d] and the 2,3-*exo*-disyndiotactic heptamer,[7] the COMPASS force field[9] as implemented into the Forcite module of ref 8 was employed. The energies of the molecular conformation adopted by the crystalline 2,3-*exo*-disyndiotactic heptamer[7] of NB and the 2,3-*exo*-diheterotactic PNB[4d] were used as reference values.

The helix shown in Figure 3 is the isolated chain model with the lowest energy we were able to obtain, i.e., only 1.6 kcal (mol monomer unit)$^{-1}$ higher than the one determined for the heptamer but 1.8 kcal (mol monomer unit)$^{-1}$ lower with respect to that of 2,3-*exo*-diheterotactic PNB. The sequence of interring torsion angles $|\theta_1|\theta_2|$ in the present case is $|169°|-129°|$, and it recalls closely values found in one of the nonterminal monomer pairs in the heptamer.[7] The relaxation of symmetry constrains did not alter either the backbone conformation or the energy of the isolated 6_1 helical chain. This result was confirmed by AM1 semiempirical calculations on chain models consisting of 24 monomers, using the GAMESS-US package.[10]

The structure of the dsPNB chain shown in Figure 3 evidences unique features which are likely to imply unique properties: the most surprising characteristic is that dsPNB chains form intramolecular tube-shaped channels which may recall some amylose and cyclodextrine type structures, albeit with the difference that the molecules and the channels in dsPNB are essentially apolar.

The 6-fold helical symmetry of the minimum energy conformation led us to the analysis of hexagonal packings which proved particularly straightforward since the 2,3-*exo*-disyndiotactic PNB chain is nondirectional, and it was therefore reasonable to assume a one-chain unit cell. Two space groups were examined, namely $P6_122$ and $P6_1$. Energy optimization of the

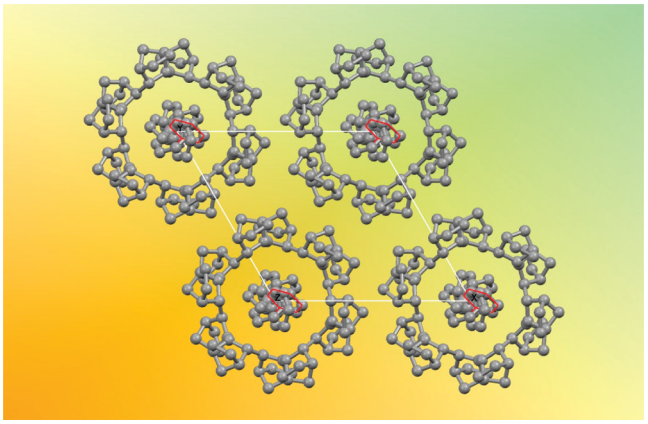

Figure 5. Projection view down the chain axis of the packing of the dsPNB−toluene containing crystal structure model obtained by rigid body Rietveld refinement against diffraction data (Figure 4). An individual toluene guest molecule is outlined with a thin red line to help recognizing it among its disordered equivalents.

packed polymer led to lattice parameters $a = b = 14.1$ Å, $c = 10.1$ Å in the case of the lower symmetry $P6_1$ space group. The minimized internal energy value was about 1 kcal (mol monomer units)$^{-1}$ higher than results obtained for 2,3-*exo*-diheterotactic PNB.[4d] The relaxation of symmetry constrains to $P1$ did not alter results significantly, and this structure represents the absolute packing energy minimum we were able to determine for dsPNB chains.

The next step in our study involved examination of the qualitative agreement between the powder diffraction profiles (not shown) calculated from the packed polymer and experimental diffraction data (Cu K_α radiation). The agreement above $2\theta = 9°$ was quite encouraging; in the pattern calculated from this model an intense 100 reflection at $2\theta = 7.3°$ is however apparent, hardly observed in experimental patterns of dsPNB (see Figure 4). The origin of the excessively strong calculated 100 reflection can be plausibly traced to the electron density modulation between the empty channels at the core of the dsPNB chains and their tightly packed walls in the structural model of infinite crystalline chains with no guests. On the other hand, we note that empty cavities are unlikely to persist in a system exposed to different types of small molecules. These considerations were sustained by thermogravimetric and spectroscopic evidence, both NMR and vibrational (see Supporting Information), confirming in many samples the presence of toluene, originating from the extraction procedure. In such samples toluene cannot be removed by keeping the samples under vacuum at 30−40 °C for a few days, which suggests that it is included into the intramolecular channels of dsPNB.

For the sake of simplicity, we will limit the discussion in the present note to models with included toluene, although it is quite apparent that other molecules may be considered as plausible guests in 2,3-*exo*-disyndiotactic PNB helices. Structural models in which the cavities are occupied by toluene were built, and the optimized molecular mechanics energies showed favorable host−guest interactions with ca. 1 toluene molecule per helical turn. The host−guest interaction energy, calculated as the difference between the energy of the host−guest system and the sum of the energies of the host (empty model) and the isolated guest molecule, leads to a packing energy more favorable by 1.5 kcal (mol monomer unit)$^{-1}$ than the empty model. In addition, the

clathrate dsPNB system is also more stable by 0.5 kcal (mol monomer unit)$^{-1}$ than crystalline 2,3-*exo*-diheterotactic PNB.[4d]

Adopting the model derived from energy optimization, which also includes the toluene guest molecule, leads to an immediate remarkable improvement of the fit between the calculated and the observed X-ray diffraction pattern, especially with respect to the reflection at $2\theta = 7.3°$. Given this fact and the highly constrained structure of the dsPNB chain, we decided to carry out the subsequent Rietveld refinement[11] with rigid body procedures. The program Debvin[12] and TOPAS-Academic[13] were used, allowing only small rotations and translations, around and along the fixed chain axis of the rigid helix containing the disordered solvent molecule (see Figure 5). Aside from the profile functions and a zero correction, the lattice parameters, the background (which models patterns of amorphous dsPNB obtained with the same synthetic approach), a unique thermal factor, the occupancy factor of the disordered toluene molecule, and coherent domains dimensions were also allowed to refine, exploring both the $P6_122$ and the $P6_1$ space groups. Since both the diffraction results and the energy calculations are significantly better for the $P6_1$ model, only the latter results are reported (see Supporting Information). A satisfactory final disagreement factor R_2' of 0.117 was obtained while refined cell parameters are $a = b = 14.10$ Å and $c = 10.44$ Å. The disagreement between the calculated and the observed pattern (see Figure 4) concentrates on some nonequatorial reflections, suggesting that disorder mainly affects the relative translations of the chains and of the guest molecules along the helix axis.

The structural refinement was carried out on the diffraction pattern (Figure 4) of a typical dsPNB toluene insoluble residue, with features intermediate between those of samples obtained in runs 1 and 2 (Table 1). The positions of the maxima correspond closely in Figures 1b and 4, and the relative intensities vary little, confirming that we are dealing with the unique crystal structure of the toluene adduct. We note however that the diffraction pattern in Figure 1b (from run 1) shows high crystallinity and peak widths almost as sharp as those of the heptamer while the pattern used for the refinement (Figure 4) shows a crystallinity of about 50% and peak widths which are also much more typical for a semicrystalline polymer.

Differences in the diffraction patterns of dsPNB could also relate, in principle, to guest exchange. While the analysis of minor intensity variations is beyond the scope of this Communication, we feel it is important to anticipate that a guest like I_2 is easily absorbed by dsPNB and influences very substantially the relative intensities in the diffraction patterns. Peak positions remain, on the contrary, invariant as expected for a unique polymer structure in which I_2 replaces toluene in the dsPNB channels.

In future work the exceptional ability of 2,3-*exo*-disyndiotactic PNB to crystallize in a unique crystal structure from degrees of polymerization around 18 upward will be discussed in more detail. Both computational and experimental investigations are being carried out to characterize the aptitude of the dsPNB chain to host different guests and optimize the morphology required to this end. The perspective is both fundamental, as the polymer presents truly unique features, and applicative with possible use in sensing and recognition/separation technologies. Synthetic work aimed at increasing the processabilty of the polymer, without losing its unique structural features, is also in progress.

■ ASSOCIATED CONTENT

Ⓢ Supporting Information. Synthetic details, GPC molecular masses, ^{13}C NMR, IR spectroscopy, TGA, details of the structural refinement procedure. This material is available free of charge via the Internet at http://pubs.acs.org.

■ AUTHOR INFORMATION

Corresponding Author

*E-mail: lido.porri@polimi.it (L.P.); valdo.meille@polimi.it (S.V.M.).

■ ACKNOWLEDGMENT

A.F., G.R., and S.V.M. acknowledge generous financial support by the CARIPLO Foundation.

■ REFERENCES

(1) (a) Janiak, C.; Lassahn, P.-G. *J. Mol. Catal. A: Chem.* **2001**, *166*, 193. (b) Blank, F.; Janiak, C. *Coord. Chem. Rev.* **2009**, *253*, 827.

(2) Sartori, G.; Ciampelli, F.; Cameli, N. *Chim. Ind. (Milan)* **1963**, *45*, 1478.

(3) (a) Kaminsky, W.; Spiel, R. *Makromol. Chem.* **1989**, *190*, 515. (b) Kaminsky., W.; Bark, A.; Arndt, M. *Macromol. Symp.* **1991**, *47*, 83. (c) Kaminsky., W.; Bark, A.; Steiger, R. *J. Mol. Catal.* **1992**, *74*, 109. (d) Kaminsky, W.; Noll, A. *Polym. Bull.* **1993**, *31*, 175. (e) Arndt, M.; Kaminsky, W. *Macromol. Symp.* **1995**, *97*, 225. (f) Arndt, M.; Gosmann, M. *Polym. Bull.* **1998**, *41*, 433. (g) Arndt, M.; Engehausen, R.; Kaminsky, W.; Zoumis, K. *J. Mol. Catal A: Chem.* **1995**, *101*, 171.

(4) (a) Haselwander, T. F. A.; Heitz, W.; Maskos, M. *Macromol. Rapid Commun.* **1997**, *18*, 689. (b) Peucker, U.; Heitz, W. *Macromol. Rapid Commun.* **1998**, *19*, 159. (c) Woodman, T. J.; Sarazin, Y.; Garrat, S.; Fink, G.; Bochmann, M. *J. Mol. Catal. A: Chem.* **2005**, *235*, 88. (d) Ricci, G.; Boglia, A.; Boccia, A. C.; Zetta, L.; Famulari, A.; Meille, S. V. *Macromolecules* **2008**, *41*, 3109.

(5) (a) Karafidilis, C.; Hermann, H.; Rufińska, A.; Gabor, B.; Mynott, R. J.; Breitenbruch, G.; Weidenthaler, C.; Rust, J.; Joppek, W.; Brookhart, M. S.; Thiel, W.; Fink, G. *Angew. Chem., Int. Ed.* **2004**, *43*, 2444. (b) Karafilidis, C.; Angermund, K.; Gabor, B.; Rufińska, A.; Mynott, R. J.; Breitenbruch, G.; Thiel, W.; Fink, G. *Angew. Chem., Int. Ed.* **2007**, *46*, 3745.

(6) Woo, T. K.; Margl, P. M.; Ziegler, T.; Blöchl, P. E. *Organometallics* **1997**, *16*, 3454.

(7) Porri, L.; Scalera, V. N.; Bagatti, M.; Famulari, A.; Meille, S. V. *Macromol. Rapid Commun.* **2006**, *27*, 1937.

(8) Materials Studio and Forcite are products of Accelrys Inc. (see www.accelrys.com).

(9) (a) Sun, H.; Rigby, D. *Spectrochim. Acta* **1997**, *A153*, 1301. (b) Sun, H. *J. Phys. Chem. B* **1998**, *102*, 7338.

(10) (a) Schmidt, M. W.; Baldridge, K. K.; Boatz, J. A.; Elbert, S. T.; Gordon, M. S.; Jensen, J. J.; Koseki, S.; Matsunaga, N.; Nguyen, K. A.; Su, S.; Windus, T. L.; Dupuis, M.; Montgomery, J. A. *J. Comput. Chem.* **1993**, *14*, 1347. (b) Gordon, M. S.; Schmidt, M. W. In *Theory and Applications of Computational Chemistry, the first forty years*; Dykstra, C. E., Frenking, G., Kim, K. S., Scuseria, G. E., Eds., Elsevier: Amsterdam, 2005; pp 1167−1189.

(11) Rietveld, H. *Acta Crystallogr.* **1967**, *22*, 151.

(12) Brückner, S.; Immirzi, A. *J. Appl. Crystallogr.* **1997**, *30*, 207.

(13) Coelho, A. A. TOPAS-Academic V4.1, 2008.